Fluoride-assisted synthesis of mullite ($Al_{5.65}Si_{0.35}O_{9.175}$) nanowires†

Yongjun Chen,*[a] Bo Chi,[b] Qiuxiang Liu,[c] Denise C. Mahon[d] and Ying Chen[a]

Received (in Cambridge, UK) 17th March 2006, Accepted 10th May 2006
First published as an Advance Article on the web 25th May 2006
DOI: 10.1039/b603999e

Novel silicon-deficient mullite ($Al_{5.65}Si_{0.35}O_{9.175}$) single crystal nanowires were synthesized in large quantities on mica substrates assisted by the intermediate fluoride species. The nanowires have diameters in the range 50–100 nm and typical lengths of several μm. Aligned nanowires were observed at the substrate edge. The nanowires have strong photoluminescence (PL) emission bands at 310, 397, 452 and 468 nm.

One-dimensional (1D) nanostructured materials have attracted great interest over the past decade due to their unique properties and potential application in the fabrication of nanoscale electronic, photonic and sensing devices.[1,2] As a result, research into the production of various nanotubes,[3–5] as well as nanowires and nanobelts,[6–11] has gained momentum. Mullite ($3Al_2O_3{\cdot}2SiO_2$) possesses relatively high chemical stability, good refractory properties and its strength can be retained up to 1300 °C.[12] This, together with excellent creep-resistance, low density, low thermal conductivity and thermal shock-resistance (due to its low coefficient of thermal expansion), makes it useful for optical applications as mid-infrared windows and an important ceramic material for electronic, optical, and high-temperature structure applications.[13–15] Mullite whiskers are an excellent reinforcement for the high-temperature ceramic composites which have been fabricated by some researchers.[16–18] Recently, hollow mullite microsized tubes and nanobelts have been successfully produced.[19,20] In this work, we report the very large scale production of silicon-deficient mullite nanowires with a composition of $Al_{5.65}Si_{0.35}O_{9.175}$. The mullite nanowires were grown on mica substrates whose main composition is Al, Si and O (Fig. S1†). Interestingly, the mullite nanowires grown at the edge of the substrate appear to be self-assembled into aligned arrays.

The growth of the mullite nanowires was carried out in a conventional tube furnace. An alumina boat loaded with ~0.1 g sodium fluoride (NaF) powder and a mica substrate was inserted into an alumina tube with NaF powder placed at the centre of the furnace. The mica substrate was located approximately 3 cm downstream of the NaF powder. The chamber was flushed with pure N_2 at a flow rate of 1000 ml min^{-1} for 30 min before the experiment commenced. Then the furnace was heated rapidly to 1100 °C under an ammonia flow (10 ml min^{-1}) and held at this temperature for 30 min. The substrate temperature was measured to be approximately 900–1000 °C. Finally, the furnace was allowed to cool down naturally to room temperature under N_2 flow (200 ml min^{-1}). The synthesized mullite nanowires were characterized by X-ray diffraction (XRD) with Cobalt Kα radiation (λ = 0.178897 nm), field-emission scanning electron microscopy (FE-SEM; Hitachi S4500), transmission electron microscopy (TEM; JEM-2010F), X-ray energy dispersive spectrometer (EDX), Raman spectroscopy (Renishaw 2000; 782 nm diode laser excitation) and photoluminescence (PL) spectroscopy (Hitachi F-4500; 255 nm excitation) at room temperature.

The SEM images of the product are shown in Fig. 1. It can be seen that very large quantities of mullite nanowires are produced and form a grass-like carpet on the mica substrate (Fig. 1a). The length of the nanowires can be up to several μm. Fig. 1b demonstrates that the nanowires appear to have a uniform diameter along their length and a clean surface. Careful observation shows that the nanowires take the shape of a pillar with a square cross-section and a faceted extremity (inset in Fig. 1b). The diameters of these nanowires are approximately 50–100 nm. The nanowires grown at the edges of the substrate can be self-assembled into aligned arrays (Figs. 1c and d). However, each nanowire has a similar morphology and diameter to those grown in the middle of the substrate. EDS results (Fig. S2†) suggest that the nanowires are composed of O, Al and a small amount of Si.

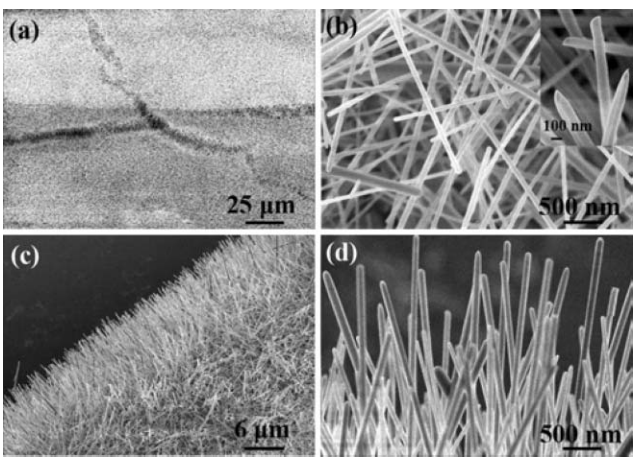

Fig. 1 (a) SEM images of the carpet-like nanowire film grown on the mica substrate. (b) Enlarged view of the nanowires. The inset shows the facet tip, smooth surface of the nanowires and diameter of approximately 50–100 nm. (c) and (d) SEM images of the aligned nanowires grown at the edge of the substrate, exhibiting similar diameters and lengths as those grown in the center of the substrate.

[a]*Department of Electronic Materials Engineering, Research School of Physical Sciences and Engineering, The Australian National University, Canberra, ACT 0200, Australia. E-mail: yong.chen@anu.edu.au; Fax: 61 2 6125 0511; Tel: 61 2 6125 8890*
[b]*National Institute of Advanced Industrial Science and Technology (AIST), 1-8-31 Midorigaoka, Ikeda, Osaka 563-8577, Japan*
[c]*School of Physics and Optoelectronic & Engineering, Guangdong University of Technology, Guangzhou, 510090, P. R. China*
[d]*Spectrochemical Laboratory, Division of Health, Science and Design, University of Canberra, ACT 2601, Australia*
† Electronic supplementary information (ESI) available: EDS results of the clean mica substrate and the product nanowires. Raman spectra of the pure substrate and mullite nanowires. See DOI: 10.1039/b603999e.

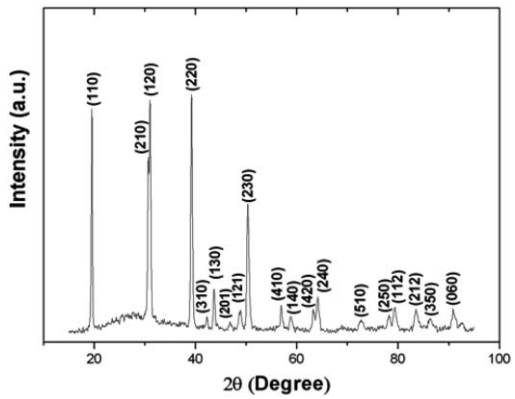

Fig. 2 XRD characterization of the nanowires.

While the relative Al and O counts are similar to those of mica (Fig. S1†), the Si component is significantly reduced, as is expected. Fig. 2 shows the XRD pattern of the synthesized nanowires. The peaks can be indexed to the orthorhombic structure $Al_{5.65}Si_{0.35}O_{9.175}$, a kind of mullite with cell parameters of $a = 7.739$, $b = 7.610$ and $c = 2.918$ Å (JCPDS No. 82-1237). No other phases are observed. It can, therefore, be concluded that the product consists of $Al_{5.65}Si_{0.35}O_{9.175}$ nanowires.

Fig. 3a shows the TEM image of a single nanowire, indicating a very smooth and clean nanowire surface, as was observed with SEM. The nanowire has a very uniform diameter of about 60 nm along its entire length. It should be noted that the black stripes are caused by the contrast difference. The corresponding selected area

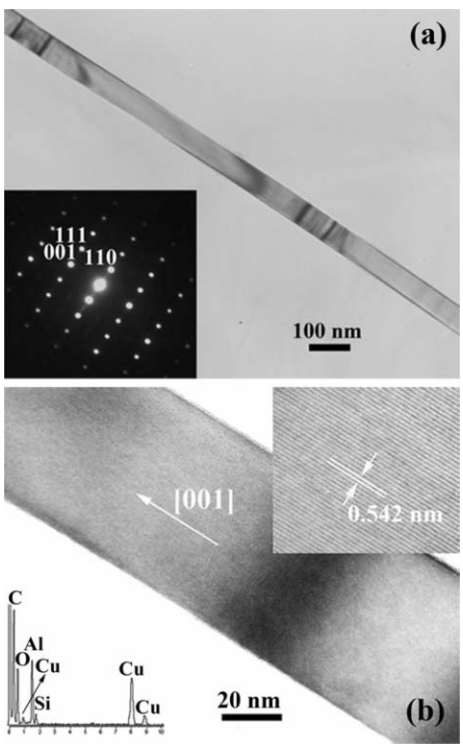

Fig. 3 (a) Low magnification TEM image of a single nanowire. The inset is the SAED pattern of the nanowire. (b) The corresponding high resolution (HRTEM) image of the same nanowire. The top-right inset is the further magnified image, while the bottom-left inset is the EDX spectrum of the nanowire.

electron diffraction (SAED) pattern (inset in Fig. 3a) can be indexed to (110), (001) planes, respectively, verifying the good crystallinity of the mullite nanowires. The high resolution TEM (HRTEM) image of this nanowire is shown in Fig. 3b. It can be observed that the lattice fringes are well defined, suggesting that the crystallinity of the mullite nanowires is perfect. The interlayer space, as is clearly shown in the top-right inset image, is approximately 0.542 nm and consistent with (110) plane lattice parameter of mullite ($Al_{5.65}Si_{0.35}O_{9.175}$). The HRTEM and SAED results indicate that the mullite nanowire grows along [001] direction. The EDX spectrum, as shown by the bottom-left inset in Fig. 3b, reveals that the nanowire mainly consists of Al, O and a very small amount of Si. The peaks of C and Cu should be attributed to the carbon film-coated copper TEM grid. This result matches the EDS result obtained under SEM very well. Further quantitative analysis shows that the atomic ratio of Al : Si : O is approximately 34.3 : 4.7 : 61.0, which is very similar to the atomic ratio for the compound $Al_{5.65}Si_{0.35}O_{9.175}$. It fits the general formula $Al_{4+2x}Si_{2-2x}O_{10-x}$ of mullites, which reveals the nanowire composition of mullite.[21]

Raman spectra were conducted for both the mica substrate and the nanowires (Fig. S3†). The peaks observed on mica substrate at frequencies of 265 cm^{-1}, 413 cm^{-1}, 644 cm^{-1}, 704 cm^{-1}, 751 cm^{-1}, 913 cm^{-1}, 952 cm^{-1} and 1115 cm^{-1} are characteristic for mica-like materials (Fig. S3a†).[22] Generally, mullite has been described as a vibrationally disordered type of sillimanite where the Al and Si atoms are randomly distributed on the tetrahedral sites. This random vibrational disorder has the effect of broadening or flattening the Raman peaks and this has been clearly demonstrated by direct comparison by Michel *et al.*[21] Bulk mullite exhibits Raman peaks with frequencies of 443 cm^{-1}, 611 cm^{-1} and 960 cm^{-1} and a high magnification ($\times 1000$) is required to collect sufficient Raman signal.[21,23] The formation of mullite nanowires present additional problems due to the scale of the incident radiation compared to the size of the surface structures. In this situation the surface would appear rough and result in a large proportion of the Raman scattering being lost. Lower signals are also expected due to the relatively low surface area density of the nanowires. Fig. S3b† shows that the nanowire surface contains broad spectral features in the region of 1100–1800 cm^{-1}. These peaks are believed to result from the bulk silicates contained in the surface layer. Most importantly, a comparison of the two traces does confirm that a significant change in the surface structure has occurred.

With the exception of Nagabhushana *et al.*, who investigated swift heavy ion bombarded mullite ($3Al_2O_3{\cdot}2SiO_2$),[24] the photoluminescence (PL) properties of mullite has not been widely reported. In this study, the PL properties of the as-synthesized mullite nanowires were measured. The results are shown in Fig. 4. Several strong PL emission bands can be observed at 310, 397, 452 and 468 nm. The origin of these PL emission peaks is not clear at the moment and there is almost no related PL literature about mullite for reference. However, it is interesting that similar PL peaks have been reported for alumina and silica nanostructures. Peng *et al.* observed PL bands at 394 nm for α-Al_2O_3 nanowires and 392 nm for α-Al_2O_3 nanobelts;[8] Wu *et al.* also observed similar PL bands in annealed porous alumina film on Si substrate.[25] They ascribed these optical transitions to the oxygen-related defects, F^+ centers (oxygen vacancies with one-electron centers). For peaks at 452 nm and 468 nm, similar results have

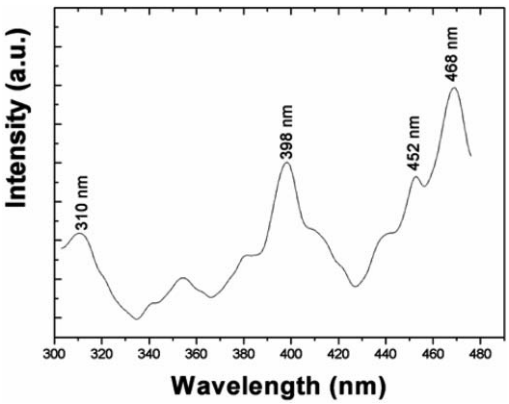

Fig. 4 Photoluminescence (PL) spectrum of the mullite nanowires.

been observed in silica nanowires and silicon oxide sheathed Si nanowires,[26,27] and oxygen vacancies exist in these nanowires have been proposed to be responsible for such PL emission. Considering that our mullite nanowires have a complex silicon-deficient composition, and the high aspect ratio of nanowires favors the formation of oxygen vacancies,[28] structural defects such as oxygen vacancy are also unavoidable. Therefore these PL emission peaks may also be attributed to the existing oxygen vacancies in the current mullite nanowires.

Given that the ends of the nanowires are facets and no droplets exist, the vapor–solid (VS) mechanism is expected to be involved in the growth of these mullite nanowires. The supposed reactions are shown in eqn (1) to (5). Ammonia decomposes into N_2 and H_2, (eqn (1)) at high temperature, and then the desired H_2O vapor for nanowire growth is created by the reaction of generated H_2 with the residual oxygen in the chamber (eqn (2)). Fluoride vapors, such as AlF_3, AlOF and HF, are then produced by the reaction of NaF with the Al_2O_3 boat (eqn (3)) in the presence of H_2O vapor, verified by the fact that the surface of the boat had changed from smooth to rough after the experiment. These fluoride vapors are then transferred downstream to the mica substrate that is located in the lower-temperature zone (approximately 900–1000 °C). HF vapor reacts with the mica substrate, resulting in continuous release of Al and Si from the substrate in the form of AlF_3, AlOF and SiF_4 vapor (eqn (4)). The vapors then precipitate on the substrate forming the mullite nuclei, as is shown in eqn (5). The relatively low rate of NH_3 flow in our experiments leads to a small vapor partial pressure and then a small supersaturation of mullite crystal, which favors the growth of the 1D nanowires rather than 3D particles. However, as mentioned above, the concentrations of AlF_3 and AlOF vapor will be much higher than that of SiF_4 vapor, as the SiF_4 vapor is generated by the already produced HF vapor. In other words, only a part of the already produced HF vapor will participate in the formation of SiF_4 vapor, while the remainder will be consumed during the formation process of mullite nanowires. As a result, Si-deficient mullite ($Al_{5.65}Si_{0.35}O_{9.175}$) nanowires, rather than normal mullite ($3Al_2O_3{\cdot}2SiO_2$) nanowires, are formed. During the whole process, the intermediate fluorides play a critical role for mullite crystal growth, which has been verified and claimed by other researchers in the case of mullite whiskers.[16,17] Actually, when no NaF starting material was used, we were unable to obtain mullite nanowires on the mica substrates. However, further investigation is needed on the growth process.

$$2NH_3(g) \rightarrow N_2(g) + 3H_2(g) \quad (1)$$

$$H_2(g) + O_2(g)(\text{residual}) \rightarrow H_2O(g) \quad (2)$$

$$6\ NaF + Al_2O_3(s) + H_2O(g) \rightarrow AlF_3(g) + AlOF(g) + 3\ Na_2O(s) + 2\ HF(g) \quad (3)$$

$$HF(g) + \text{mica(Al–Si–O)} \rightarrow AlF_3\ (g) + AlOF(g) + SiF_4(g) + H_2O(g) \quad (4)$$

$$AlF_3(g) + 4.65\ AlOF(g) + 0.35\ SiF_4(g) + 4.525\ H_2O(g) \rightarrow Al_{5.65}Si_{0.35}O_{9.175}\ (\text{nanowires}) + 9.05\ HF(g) \quad (5)$$

The authors acknowledge financial support from the Australian Research Council (ARC) Discovery-Projects grant (No. DP0452249) and thank Dr Sally Stowe and the staff of the Electron Microscopy Unit for the use of various microscopy facilities.

Notes and references

1 Y. Cui, Q. Q. Wei, H. K. Park and C. M. Lieber, *Science*, 2001, **293**, 1289.
2 F. Favier, E. C. Walter, M. P. Zach, T. Benter and R. M. Penner, *Science*, 2001, **293**, 2227.
3 S. S. Fan, M. G. Chapline, N. R. Franklin, T. W. Tombler, A. M. Cassell and H. J. Dai, *Science*, 1999, **283**, 512.
4 Y. Chen, L. T. Chadderton, J. F. Gerald and J. S. Williams, *Appl. Phys. Lett.*, 1999, **74**, 2960.
5 M. Remskar, A. Mrzel, Z. Skraba, A. Jesih, M. Ceh, J. Demsar, P. Stadelmann, F. Levy and D. Mihailovic, *Science*, 2001, **292**, 479.
6 Z. W. Pan, Z. R. Dai and Z. L. Wang, *Science*, 2001, **291**, 1947.
7 Y. J. Chen, J. B. Li and J. H. Dai, *Chem. Phys. Lett.*, 2001, **344**, 450.
8 X. S. Peng, L. D. Zhang, G. W. Meng, X. F. Wang, Y. W. Wang, C. Z. Wang and G. S. Wu, *J. Phys. Chem. B*, 2002, **106**, 11163.
9 Y. D. Yin, Y. Lu, Y. G. Sun and Y. N. Xia, *Nano Lett.*, 2002, **2**, 427.
10 M. C. Johnson, C. J. Lee, E. D. Bourret-Courchesne, S. L. Konsek, S. Aloni, W. Q. Han and A. Zettl, *Appl. Phys. Lett.*, 2004, **85**, 5670.
11 T. Kuykendall, P. Pauzauskie, S. K. Lee, Y. F. Zhang, J. Goldberger and P. D. Yang, *Nano Lett.*, 2003, **3**, 1063.
12 H. Schneider, K. Okada and J. Pask, *Mullite and Mullite Ceramics*, Wiley, Chichester, 1994.
13 I. A. Aksay, D. M. Dabbs and M. Sarikaya, *J. Am. Ceram. Soc.*, 1991, **74**, 2343.
14 M. A. Camerucci, G. Urretavizcaya, M. S. Castro and A. L. Cavalieri, *J. Eur. Ceram. Soc.*, 2001, **21**, 2917.
15 R. R. Tummala, *J. Am. Ceram. Soc.*, 1991, **74**, 895.
16 P. Peng and C. Sorrell, *Mater. Lett.*, 2004, **58**, 1288.
17 H. J. Choi and J. G. Lee, *J. Am. Ceram. Soc.*, 2002, **85**, 481.
18 L. B. Kong, H. Huang, T. S. Zhang, Y. B. Gan, J. Ma, F. Boey and R. F. Zhang, *Mater. Sci. Eng., A*, 2003, **359**, 75.
19 X. Y. Kong, Z. L. Wang and J. S. Wu, *Adv. Mater.*, 2003, **15**, 1445.
20 B. Zhang, C. B. Cao, X. Xiang and H. S. Zhu, *Chem. Commun.*, 2004, 2452.
21 D. Michel, P. H. Colomban, S. Abolhassani, F. Voyron and A. Kahn-Harari, *J. Eur. Ceram. Soc.*, 1996, **16**, 161.
22 D. A. McKeown, M. I. Mell and E. S. Etz, *Am. Mineral.*, 1999, **84**, 1041.
23 N. Q. Liem, G. Sagon, V. X. Quang, H. V. Tan and P. H. Colomban, *J. Raman Spectrosc.*, 2000, **31**, 933.
24 H. Nagabhushana, B. N. Lakshminarasappa, F. Singh and D. K. Avasthi, *Nucl. Instrum. Methods Phys. Res., Sect. B*, 2003, **211**, 545.
25 J. H. Wu, X. L. Wu, N. Tang, Y. F. Mei and X. M. Bao, *Appl. Phys. A: Mater. Sci. Process.*, 2001, **72**, 735.
26 D. P. Yu, Q. L. Hang, Y. Ding, H. Z. Zhang, Z. G. Bai, J. J. Wang, Y. H. Zou, W. Qian, G. C. Xiong and S. Q. Feng, *Appl. Phys. Lett.*, 1998, **73**, 3076.
27 J. F. Qi, J. M. White, A. M. Belcher and Y. Masumoto, *Chem. Phys. Lett.*, 2003, **372**, 763.
28 C. H. Liang, G. W. Meng, Y. Lei, F. Phillipp and L. D. Zhang, *Adv. Mater.*, 2001, **13**, 1330.

